

**OMAE2008-57246**

## **ADDED RESISTANCE OF MOONPOOLS IN CALM WATER**

**Riaan van 't Veer**

GustoMSC  
Hydrodynamic and Stability Department  
Schiedam, The Netherlands

**Haye Jan Tholen**

Delft University of Technology  
Department of Marine Technology  
Delft, The Netherlands

### **ABSTRACT**

The additional ship resistance due to water oscillations in an open moonpool as constructed in drillships can be obtained through model tests. The oscillation has a dominant frequency and character, and the amplitude increases with forward speed. The resonant oscillation mode can be piston or sloshing. Recent measurements show that both types of oscillation can increase ship resistance to the same magnitude. The sloshing mode dominates in longer moonpools, while piston mode oscillations are dominant in shorter moonpools. Based on two model tests series carried out at Delft University of Technology, a resistance prediction model is constructed for piston type oscillations. The model was verified with a resistance measurement performed at MARIN in the past, showing fair agreement between the predicted and measured resistance increase.

### **KEYWORDS**

Moonpool, drillship resistance, prediction model

### **INTRODUCTION**

GustoMSC has been one of the leading designers and former builder of DP drillships since the early 1970's, when the first dynamically positioned drillship, the "Pelican", went into service in 1972. At that time the drillships were equipped with two moonpools: an almost square drilling moonpool and a separate small ROV moonpool. The trend in current drillship design is to lengthen the moonpool to allow dual operation in one single moonpool, and the small ROV moonpool is often not present anymore. Current industry practice is to design rectangular shaped moonpools.

The global dimensions of the moonpool are an important design parameter from an operational perspective, but as well from a hydrodynamic viewpoint. Depending on the length to draft ratio, vertical moonpool water column oscillations can be excessive at forward speed. Theoretically, the moonpool geometry determines the piston and sloshing resonant

frequency, while the speed determines the oscillation amplitude. Due to the phase locking phenomenon the violent resonant mode oscillation is sustained over a large speed regime.

Research in the past demonstrates that there is a direct correlation between the vertical (piston) moonpool water motion amplitude and the added resistance at speed. The added resistance increase can be considerable (up to 30% at moderate forward speed), reducing the transit speed or increasing fuel consumption.

To study the added resistance due to a moonpool in a modern drillship, model tests (scale 1:50) are performed at the TU Delft Ship Hydromechanics Laboratory, both in 2007 and in 2000. This paper presents and discusses the results of both experimental research programs. The results show the effect of the moonpool length and draft on resistance, and the influence of several resistance mitigation devices. Based on the model test data, an added resistance prediction model is constructed which can be of guidance for future moonpool design.

### **MOONPOOL GEOMETRY AND DIMENSIONS**

The length and width of a moonpool are derived from operational and structural requirements. The moonpool draft equals the draft of the vessel which follows from operational and stability requirements.

The location of the moonpool in the ship will generally be around midship which allows good structural integration, efficient DP power consumption, and minimizes relative heave motion compensation.

The width of a moonpool must be wide enough to ensure that the riser remains free of the moonpool sides under ship motions, and must allow running of subsea equipment. The location of the diverter above keel defines the point from where the riser departure angle in ship fixed reference system is measured. Generally, a roll angle of about 10 degrees (amplitude) should be allowed for. Operability calculations are performed to verify workability in an early design stage. Hull

structural requirements can limit the moonpool width and impose requirements on how the moonpool is integrated in the ship, in particular near the ship keel.

The length of the moonpool is based on the same requirement that the riser should remain free of the fore and aft moonpool wall, from which pitch motion limits are defined. Another moonpool length requirement arises from the type of operation to be carried out. Dual drill operations require a moonpool of about twice the length as for single drill operation. The current moonpool designs often originate from experiences with previous vessels and owner specific requirements.

In Table 1 an overview is given of moonpool dimensions in by others and GustoMSC designed vessels.

**Table 1: Overview of several drillship designs**

Design	Year	Ship dimensions		Moonpool dimensions	
		LOA [m]	B [m]	L [m]	B [m]
<i>GustoMSC designs:</i>					
Pelican class	1972	147.70	27.00	7.20	8.20
Pride Africa / Angola	1999	204.52	29.87	12.01	10.00
GSF C.R.Luigs / J. Ryan	2000	231.34	35.97	12.80	12.80
Gusto WIV	2004	127.40	24.00	9.60	9.00
PRD12k - Oribis	2007	156.00	29.90	16.90	10.40
PRD12k - Bully	2007	166.50	32.00	19.60	12.60
<i>Not designed by GustoMSC:</i>					
Deepwater Expedition	1989	171.00	28.40	8.53	8.00
Deepwater Frontier	1999	221.28	42.06	14.63	14.63
Deepwater Pathfinder	1999	221.28	42.06	25.60	12.40
Discovery Enterprise	1999	254.51	38.10	24.38	9.41
Deepwater Discovery	2000	227.38	42.06	18.37	12.47
Saipem 10000	2000	227.00	42.00	25.60	10.26
Belford Dolphin	2000	204.80	39.90	24.38	10.06
Chikyū	2005	210.00	38.00	22.00	12.00

Most of the drill ships reach a transit speed in the range of 10 to 12 knots, without excessive moonpool resonance. Often model tests are performed to verify this in the design phase. The economical balance between additional power for higher transit speed and resulting shorter transit time needs to be investigated, but it is outside the scope of the presented paper. The quest for higher forward speed in combination with the unknown additional added resistance of longer moonpools ( $L/B > 1.5$ ) was the main motivation for performing an additional model test series. The tests performed in 2000 by Cotteleer [7] hold valuable information on moonpools with  $L/B=1$  and varying draft to beam ratios ( $0.39 < D/B < 0.78$ ). Larger  $L/B$  ratios were not tested at that time. The test series of 2007 by Tholen [8] provides additional trends up to  $L/B=2$ , and in addition focus on resistance mitigation devices to reduce additional transit vessel resistance.

## HULL AND MOONPOOL RESISTANCE

The installed power in a drillship is mainly determined from the dynamic positioning (DP) requirements, since most of time the vessel is stationary. Environmental forces for DP assessment in an early design loop include wave drift forces

based on 3D potential flow calculations, current forces from model tests or calculated data, and wind forces based on model tests or from WINDOS calculations. In all force contributions the influence of the moonpool is considered to be small.

The resistance curve prediction in an early design phase relies mostly on scaled model tests in combination with experiences based on previous designs. Unfortunately, an accurate estimate of the added resistance contribution from the moonpool remains difficult, while its magnitude can be significant. The variation in hull and moonpool designs is large and the available test data is often too limited for an accurate trend prediction. With this in mind, the tests series of Cotteleer [7] were extended by Tholen [8] to obtain a systematic moonpool series which enables derivation of an empirical resistance prediction tool.

Although the moonpool geometry is in essence very simplistic, most often rectangular shaped with vertical walls, the associated flow phenomena are far from that. The general consensus is that the water column oscillations inside the moonpool are the major cause for the resistance increase, which is denoted as ‘cavity drag’ [1] in literature. This drag also exists for closed cavities (a cavity without free surface, or lid-driven cavities) which are often studied experimentally and by modern CFD tools (for low Reynolds numbers). The existence of the free surface in the moonpool and the large Reynolds numbers are factors that complicate application of CFD tools.

Moonpool resonant oscillations are initiated by vortices that start at the upstream submerged moonpool edge. The vortices are related to the separation of a shear layer [9] so viscous effects dominate the initiation and possibly as well the flow pattern in the moonpool. The geometry of the moonpool defines theoretical piston and sloshing resonant modes with associated frequencies.

To suppress resonant moonpool behaviour two possible solutions are considered: either the cause of the vortex creation is reduced, or the consequence of it, the large water column oscillation, is reduced.

Viscous damping and sloshing suppression devices have been studied and applied since long to reduce free surface oscillations. A comprehensive review can be found in Ibrahim [2]. Baffles, floating lids or mats are a few examples. Aalbers [10] and Fukuda [4] carried out experiments with horizontal damping plates, both showing that the most effective location being higher up in the moonpool. Longitudinal sloshing can be reduced by partitioning the tank to reduce the possible run length of the waves and to de-tune natural periods; a well-known solution in tanks of oil and LNG carriers. Flow intervening devices, like damping plates, near the free surface reduce the wave oscillations, but the vortex generation at the moonpool leading edge still takes place. The cavity-vortex reduces only by the fact that the recirculation of vortices in the moonpool reduces. Recirculation of the vortices is initiated by the impingement of vortices at the downstream moonpool wall. The vortex can either curve upwards towards the free surface, or is shed in the wake underneath the hull.

The design of the mitigation devices as used by Tholen [8] are based on two principles: to decrease the vortex sheet generation at the leading edge and/or to reduce the (upwards) mass flux at the downstream wall (that is to reduce the cavity-vortex recirculation). For example, a traditionally applied wedge underneath the moonpool leading edge curves the flow outwards intending to carry vortices away underneath the vessel by the forward speed. In the experience of GustoMSC, the wedge is effective for short moonpools, but fails to reduce the resistance for longer moonpool designs. The possible reduced moonpool oscillation resistance does not balance the increased hull resistance due to the appended wedge. Little is known on how to design a most efficient wedge.

### MODEL TEST CAMPAIGN '2000'

Model tests for a drillship of 210 m length at scale 1:50 were performed by Cotteleer [7] at Delft University of Technology. The model was fitted with a rectangular moonpool. The model was free to heave and pitch, but restrained in all other directions. Inside the moonpool three wave probes were installed along the centerline. The resistance of the model in calm water was measured by two force transducers fitted between the model and the carriage.

The geometry ratio of the moonpool was  $L/B = 1.0$  and three draft to beam ratios were tested:  $D/B = 0.39, 0.59$  and  $0.78$ . The speed range of the test with the shallow draft went up to Froude number  $Fn = 0.265$ , and for the two other drafts up to  $Fn = 0.214$  (where  $Fn$  is based on the ship's length).

### MODEL TEST CAMPAIGN '2007'

Model tests for the same drillship as used in 2000 were conducted by Tholen [8] at Delft University of Technology. A new model was constructed, scale 1:50, with a moonpool of identical width as in 2000.

Three different moonpool length variations were tested with  $L/B$  ratio of 1.0, 1.5 and 2.0. The upstream edge had a fixed location in the model. The draught was kept constant in all tests with ratio  $D/B = 0.70$ .

The vessel was tested in calm water conditions up to Froude number (based on length) 0.210. The model was free to heave and pitch. To investigate the influence of ship motions, two runs at different forward speed were performed with a captive model for each configuration. In those runs the model sinkage and trim was according the means of the 'free' sailing test.

The following data was measured: resistance by means of force transducers, water motions inside the moonpool by means of wave probes and ship motions by means of the optical KRYPTON system. Video recordings were made from each run capturing the water surface motions inside the moonpool.

The influence of four different resistance mitigation devices was measured at  $L/B=1$  and  $L/B=2$ . The variations are presented in Figure 1 and described by (top to bottom): A) the influence of a wedge at the upstream end and an additional cut-out at the downstream edge, B) the influence of an intermitted

wedge at the moonpool upstream edge, C) the influence of a converging moonpool bottom, and D) the influence of an inward sloped aft moonpool wall.

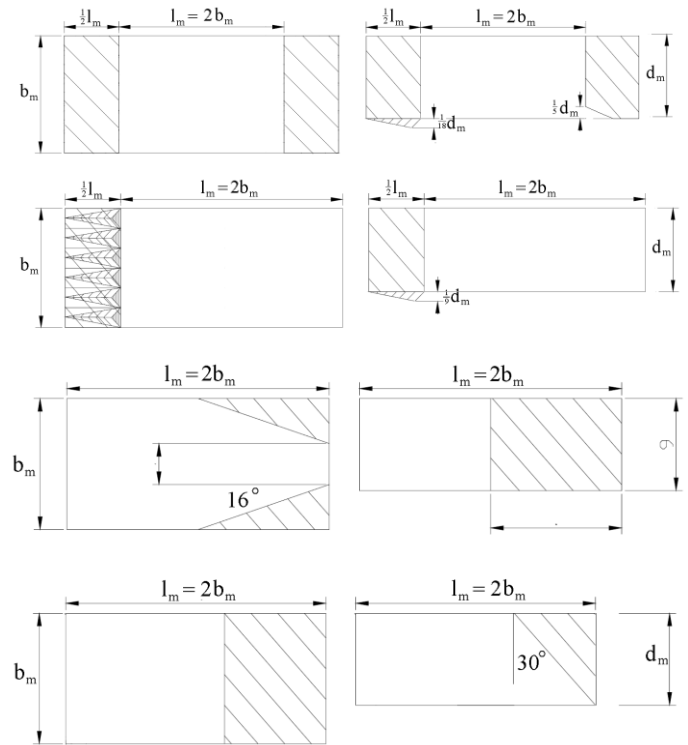


**Figure 1: Four different moonpool variations as used in the 2007 experiments. Bottom view to the left, and side view to the right.**

### MOONPOOL RESISTANCE

The added resistance contribution due to the moonpool could be deduced since the overall model resistance was also measured with a bottom closed moonpool. The measured model scale data is extrapolated to full scale, and the results from 2000 and 2007 are presented as resistance coefficient increase  $\Delta CTS$  defined by:

$$\Delta CTS = \frac{R_{\text{With Moonpool}} - R_{\text{No Moonpool}}}{1/2\rho U^2 A_m} \quad (1)$$

in where the moonpool area is  $A_m = l_m b_m$ , with moonpool length  $l_m$ , and moonpool width  $b_m$ . The resistance coefficient is found to increase linearly with the ratio of significant moonpool resonant amplitude  $A_{1/3}$  over moonpool draft  $d_m$ . Figure 2 includes the results from all performed tests series (2000 and 2007), with and without resistance mitigation devices. Note that the data is obtained for rectangular moonpools with equal width and varying  $l_m/b_m$  and  $d_m/b_m$  ratios as described above.

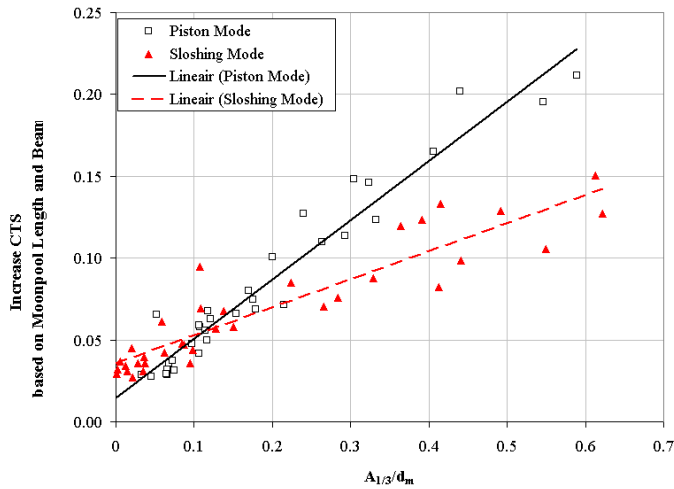


**Figure 2: Resistance increase ( $\Delta CTS$ ) versus measured water level oscillation amplitude (significant  $A_{1/3}$ )**

The significant moonpool resonant amplitude is obtained by averaging the significant water elevation amplitude obtained from all individual wave elevation recordings inside the moonpool when in piston resonance, and is the average from the aft and front water level elevation when in sloshing mode.

The two resonant modes show a different dependency. The resistance increase due to piston oscillation is stronger given the same wave amplitude/draft ratio than for sloshing. The interception of the sloshing trend line at zero water oscillations ( $\Delta CTS(A_{1/3}/d_m = 0)$ ) is above the piston trend line intersection since the most significant sloshing amplitudes were obtained with the longer moonpool ( $L/B=2$ ) that in itself has a larger added resistance than the shorter moonpools for which only significant piston mode oscillations were measured.

Significant time varying resistance was measured in each test run. The frequency of this variation was equal to the dominant frequency measured in the water level oscillations inside the moonpool, confirming the correlation between moonpool water oscillations and resistance.

In Figure 3 the resistance increase due to the moonpool is given for the three rectangular open moonpools at  $D/B=0.70$  and for the best resistance mitigation device tested as function of forward speed. The dominate oscillation mode of the water column is given by P=piston, S=sloshing, n=no dominate mode. The contribution of the moonpool to the overall resistance is significant and can be summarized as follows:

- $L/B=1$ : The dominant mode is piston oscillation. The resistance peak is at  $Fn=0.15$  showing about 60% added resistance. At increasing speed the added resistance drops rapidly to about 10%. Mitigation devices A, B and C all reduced the resistance considerable, but in particular device A and C. The results for the wedge/cut-out moonpool (A) are presented.

- $L/B=1.5$ : The moonpool oscillations start in sloshing mode, but soon transits to piston mode. At low forward speed resistance increase is about 30%. When forward speed increases above  $Fn=0.13$ , resonant behaviour picks up and the resistance becomes twice as large at  $Fn=0.20$  as for the closed moonpool situation. No devices were tested.
- $L/B=2$ : Only sloshing mode oscillations were measured. At low forward speed the resistance increase is about 50%. Above  $Fn=0.15$  the resistance increases sharply to twice as large at  $Fn=0.20$  as for the closed moonpool. The converging moonpool (C) but in particular the aft sloped moonpool (D) show significant resistance reduction.

We note that the hull lines of the vessel were not optimized for high forward speed.

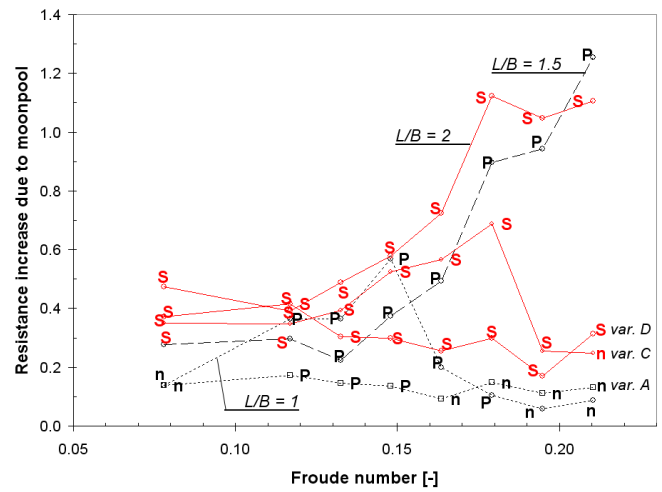


**Figure 3: Resistance increase for several moonpool configurations with oscillation mode piston (P) or sloshing (S) or none (n).**

### MOONPOOL OSCILLATION FREQUENCY

The two distinct moonpool resonance modes, vertical heaving or piston mode and longitudinal surging or sloshing mode could be clearly observed in the experiments. Transverse swaying of the water surface was not observed, neither were strong three dimensional effects visible.

Figure 4 shows piston mode water oscillations (left part) for the  $L/B=1.5$  moonpool at 17.18 knots ( $Fn=0.19$ ) and sloshing mode oscillations (right part) for the  $L/B=2$  moonpool at the same speed. At this particular speed the  $L/B=1$  moonpool did not exhibit resonant behaviour anymore.

In piston mode the major part of the surface moves up and down over the whole moonpool area. The water surface does not remain completely horizontal and longitudinal water flow velocities are present. The same observation was described by English [3]: the water level rises at the aft end of the moonpool up to point located near the front end of the moonpool (see photos 1 and 2 in Figure 4 of piston mode series). When the

mean water level goes down (photo 3), this stagnation boundary visibly moves more forward. It re-appears at the aft when the water level rises again (photo 1). In sloshing mode (left series of photos in Figure 4) a clear crest and trough are seen at the same time at the aft and forward moonpool wall (photos 1 and 4). The water motions at the aft and front move out of phase to each other. The water level in the middle of the moonpool remains relatively at the same level at all times.

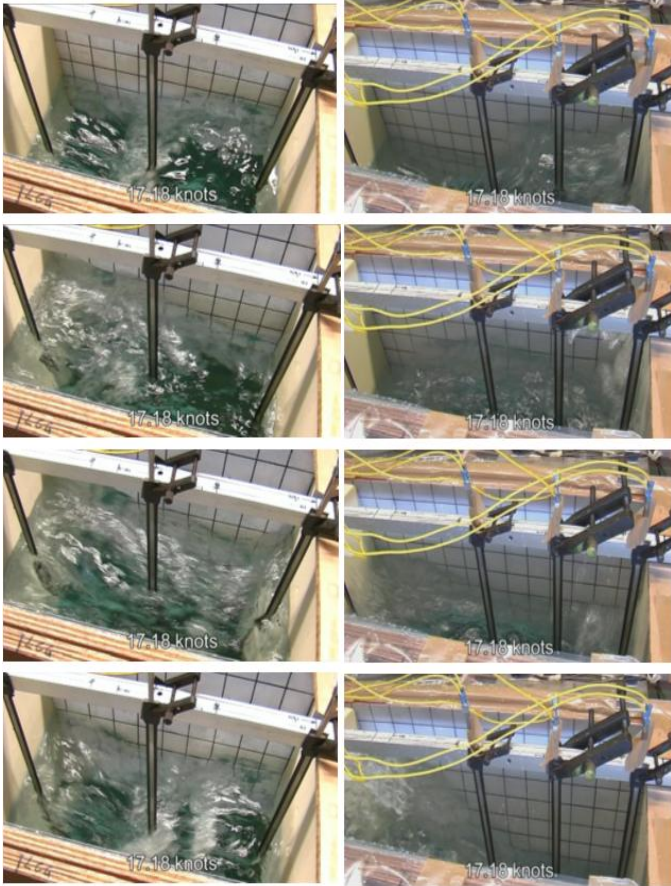


**Figure 4: Piston mode for the L/B=1.5 moonpool (left figure) and sloshing mode for the L/B=2 moonpool (right figure), both at 17.18 knots forward speed. Sailing direction is to the right in the photo series.**

The natural periods of the first piston and sloshing mode of a moonpool can be predicted based on the overall length, beam and draft (assuming rectangular moonpools). Assuming a single degree of freedom heave motion equation:

$$(m+m')\ddot{z}+b\dot{z}+cz=F(t) \quad (2)$$

the natural undamped frequency for this system represents the piston mode natural frequency of the moonpool water column:

$$\omega_n = \sqrt{\frac{c}{m+m'}} \quad (3)$$

where  $m$  is the mass of water inside the moonpool,  $m'$  is the added mass and  $c$  is the spring constant. Since the spring constant of the moonpool and the mass can be obtained through the length, beam and draft, the natural piston mode frequency can also be written as:

$$\omega_n = \sqrt{\frac{g}{d_m+d'_m}} \quad (4)$$

where  $d_m$  is the moonpool draught and  $d'_m$  the added draught due to added mass. Fukuda [4] presents an empirical added draught:

$$d'_m = 0.41\sqrt{S_m} \quad (5)$$

where  $S_m$  is the moonpool plane area. The factor 0.41 was obtained from experiments with a large number of different moonpool geometries, rectangular and circular. A theoretically based formulation is derived by Molin [5]. He formulated the flow field for a three-dimensional moonpool by a velocity potential with appropriate boundary conditions, leading to:

$$d'_m = \frac{b_m}{\pi} \left\{ \operatorname{asinh}\left(\frac{l_m}{b_m}\right) + \frac{l_m}{b_m} \operatorname{asinh}\left(\frac{b_m}{l_m}\right) + \frac{1}{3} \left( \frac{b_m}{l_m} + \frac{l_m^2}{b_m^2} \right) - \frac{1}{3} \left( 1 + \frac{l_m^2}{b_m^2} \right) \sqrt{\frac{b_m^2}{l_m^2} + 1} \right\} \quad (6)$$

Both the piston and sloshing natural frequency are valid for an undamped system, and assume a frequency independent added mass. Comparing equation (5) and (6) reveals that the added mass in Molin's formulation is larger than in Fukuda's, leading to lower natural frequencies. Table 2 shows the piston natural frequencies for several moonpool geometry ratios as observed in the model tests.

The natural sloshing mode of a moonpool can be derived assuming a standing wave in longitudinal direction. A formulation for the  $n$ -the sloshing mode can be found in for example Newman [6] or Fukuda [4]:

$$\omega_L = \sqrt{\frac{n\pi g}{l_m}} \quad (7)$$

where  $n=1$  represents the first sloshing natural frequency. Molin [5] presents a more complicated formulation, based on

the derivation of a velocity potential, which include the moonpool draft:

$$\omega_L \cong \sqrt{\frac{n\pi g}{l_m} \cdot \frac{1 + J_{n0} \tanh(n\pi d_m / l_m)}{J_{n0} + \tanh(n\pi d_m / l_m)}} \quad (8)$$

where  $J_{n0}$  involves an integral over the moonpool length and beam which can be obtained through numerical integration. Table 3 shows the sloshing natural periods for several moonpool geometry ratios as used in the model tests.

**Table 2: Piston mode natural frequencies**

Moonpool geometry ratio		Piston Natural Frequency [rad/s]	
$l_m / b_m$	$d_m / b_m$	Fukuda, eq. (5)	Molin, eq. (6)
1.0	0.3906	0.9784	0.9419
1.0	0.5859	0.8772	0.8507
1.0	0.7031	0.8298	0.8072
1.5	0.7031	0.7974	0.7747
2.0	0.7031	0.7729	0.7525

**Table 3: Sloshing mode natural frequencies**

Moonpool geometry ratio		Sloshing Natural Frequency [rad/s]	
$l_m / b_m$	$d_m / b_m$	Newman, eq. (7)	Molin, eq. (8)
1.0	0.3906	1.5517	1.5844
1.0	0.5859	1.5517	1.5612
1.0	0.7031	1.5517	1.5562
1.5	0.7031	1.2669	1.2864
2.0	0.7031	1.0972	1.1376

As noted by Molin, the natural frequency of the first sloshing mode is always higher than the first piston mode. For longer moonpools both frequencies are closer to each other than for shorter moonpools, which is observed in Figure 5. The experimental data in Figure 5 is obtained from different moonpool geometry ratios and at different forward speeds.

The water elevation oscillatory frequencies in the experiments are obtained from statistical post-processing. The wave elevation spectrum often shows multiple peaks, of which one dominates significantly. This frequency determines the mode of oscillation of the moonpool and is presented in Figure 5. The natural frequencies of the piston and sloshing mode are clearly observed and do match the predictions well. The measured piston frequencies for the shortest moonpool show the largest scatter in the experiments, but at this frequency most data points are found as well. The longer moonpool shows a tendency to oscillate more often in sloshing mode than in piston mode, and again some scatter is observed.

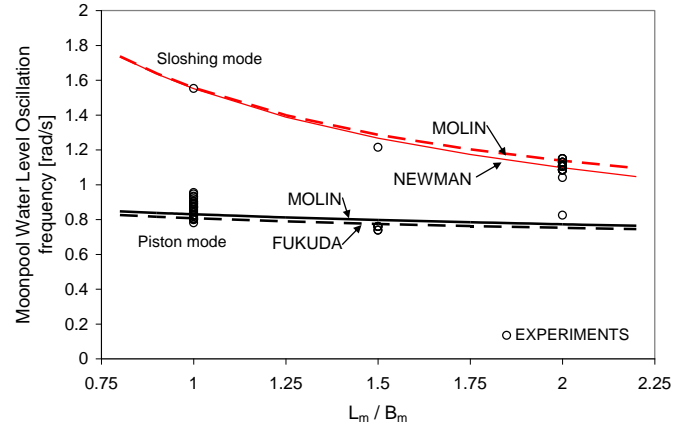


**Figure 5: Oscillation frequency of water level inside moonpool**

### MOONPOOL EXCITATION

Many researchers describe the initiation of water level oscillations in a cavity due to constant on-set flow ([1], [3], [4]). The general consensus is that vortices originate from the turbulent boundary layer at the upstream end of the moonpool, and if these vortices are of sufficient strength they initiate new vortices via flow re-circulation inside the moonpool. The re-circulation exists and is self-sustained due to the presence of the downstream wall of the moonpool. At this downstream wall the flow impingement causes large pressure fluctuations, since the impingement point varies in location by the fact that the shear layer is turbulent. Rockwell and Naudascher [9] describe this phenomenon in detail, for cavities without free-surface (no fluid-air boundary). The fluid re-entrained into the cavity disturbs the shear-layer at the upstream edge, which leads to a self-exciting feed-back mechanism of vortex generation.

The excitation frequency is considered to be a function of the forward speed of the vessel that is the flow speed over the cavity. With increasing speed or increasing cavity length, the shear layer vortices grow and this can introduce a cavity-vortex between the moonpool free-surface and the instable shear layer at keel level. This cavity-vortex is considered to rotate inside the moonpool and if of sufficient strength, it reaches the upstream moonpool boundary, disturbing the shear layer. Thereby a self-excitation mechanism exists. If the moonpool damping is low, it can start a piston or sloshing mode oscillations at a resonant frequency. At this point the excitation mechanism changes because it is now dominated by the oscillation itself. The vortices generated at the leading edge have the same frequency of the oscillating water column. Fukuda [4] observed a variation of this frequency around the calculated theoretical moonpool resonant modes and attributed this to phase locking: the oscillations of the moonpool water column become so large that they control the creation of new vortices and lock the system at this frequency when speed increases. In model tests we observed the growing resonant

amplitudes when the vessel was already some time at its requested speed, which supports the phenomenon described above. It confirms the idea that a certain amount of time or run length is required before the self-excitation vortex stabilizes.

The vortex shedding from objects relates to the Strouhal number  $St$  defined as:

$$St = \frac{f_s l_m}{U} \quad (9)$$

where  $f_s$  is the frequency of vortex shedding,  $l_m$  the impingement length (moonpool length), and  $U$  the flow velocity (forward speed). The relationship between the Reynolds number (model scale) and the measured Strouhal number (based on the water level oscillation frequency) is given in Figure 6. The Strouhal number ( $St$ ) is not constant with Reynolds number, but of similar order as for vortex shedding from circular cylinders with turbulent boundary layer (0.2-0.4). The sloshing mode frequency is about 1.5 times the piston mode frequency, and this is reflected in the Strouhal numbers (for  $L/B=2$ ).

Although we will not further discuss the resistance variations in this paper, an important observation is that the measured resistance of the model was found to fluctuate with the same frequency (Strouhal number) as the water level oscillations. The variations are of significant magnitude, as reported by English [3] as well.

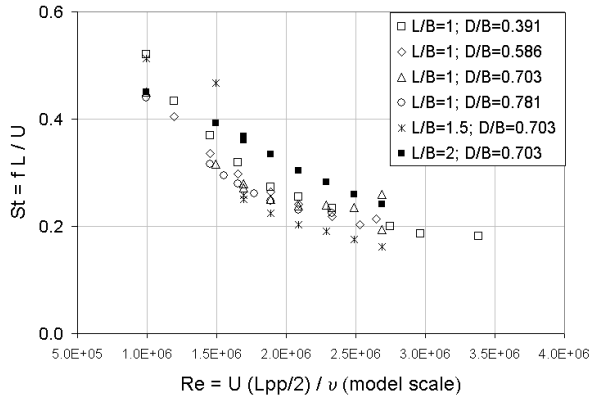


**Figure 6: Strouhal versus Reynolds numbers for several rectangular moonpools**

### MOONPOOL OSCILLATION AMPLITUDE

The piston mode oscillation amplitudes over draft,  $A_{1/3}/d_m$ , versus draft over beam ratio are given in Figure 7. The data refers to the open moonpools without any resistance mitigation devices. The trend is that with increasing vessel draft the oscillation amplitudes reduce linearly. All data points except the solid triangular points are obtained with  $L/B=1$ . The triangular points are measured at  $L/B=1.5$ , and at maximum forward speed in the test the maximum oscillation amplitude

was found. In other words, the possible peak resonant amplitude for piston mode was not measured. For all other measurement series, the peak value was found.

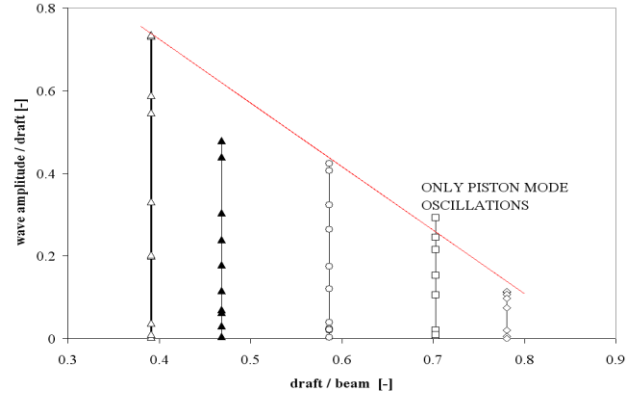


**Figure 7: Piston mode water oscillation amplitudes in clean moonpools.**

In Figure 8 the non-dimensional oscillation amplitudes are given as function of the inverse Strouhal number (based on the theoretical piston resonant frequency in [rad/s]) or reduced velocity number. Remarkable is that the slope of the amplitude increase remains constant up to the maximum resonant amplitude. The increase is also independent of the  $D/B$  and  $L/B$  ratio. A striking observation is that all oscillations start at a reduced velocity of 0.35 and at 0.85 all oscillations vanish. The above is also visible in Figure 9 where the influence of three resistance mitigation devices on the water level (piston) oscillations is presented.

With increasing draft at the same  $L/B$  ratio, the decline of the water oscillation amplitudes after the peak value becomes less sharp, which is also true for the different mitigation devices. The influence of the mitigation device is furthermore that the slope of the water level amplitude increase versus reduced velocity is different than for the clean moonpools.

Following the work of Fukuda [4] and Aalbers [10] the motion equation for an oscillating water column (piston mode) can be written as:

$$(d + d') \frac{d^2 z}{dt^2} + k_1 \frac{dz}{dt} + k_2 \frac{dz}{dt} \left| \frac{dz}{dt} \right| + gz = V_e(t) \frac{dz}{dt} \quad (10)$$

where  $V_e(t)$  is the velocity associated with the excitation mechanism. Using the momentum theorem, Fukuda derived an expression for the vertical water oscillations:

$$\frac{A}{l_m} = \frac{3\pi}{16} \frac{U - U'}{(2k_2)l_m \omega} \quad (11)$$

where  $A$  is the oscillation amplitude,  $U$  the onset velocity,  $U'$  the velocity where oscillation start, and  $k_2$  is a non-linear damping coefficient including the area at the moonpool free surface and keel,  $k_2 = (1/2)(S_{top}/S_{bottom})^2 = 1/2$  for rectangular moonpools. The damping value  $k_2$  determines the slope of the moonpool amplitude increase, and this confirms our finding as presented in Figure 9. The amplitude increase for rectangular clean moonpools, following Fukuda's estimated equation (11), is added to Figure 8, and it matches the data well. The linear increase is by a factor  $3\pi/16 \approx 0.589$ . The onset velocity is found to correlate with  $(1/St) = 0.35$ .

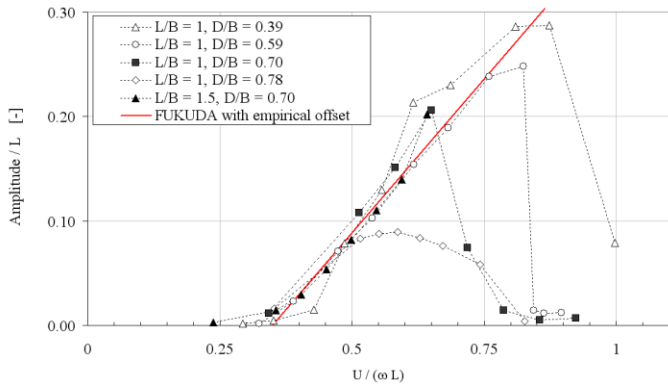


**Figure 8: Piston mode water oscillation amplitudes versus inverse Strouhal number**

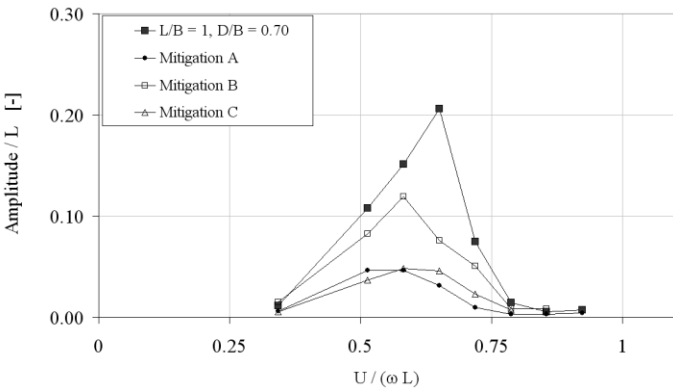


**Figure 9: Influence of resistance mitigation devices on moonpool oscillation amplitudes**

### 'PISTON' ADDED RESISTANCE PREDICTION MODEL

Combining the data presented above, a prediction model for piston type oscillation and resulting vessel added resistance is derived. The prediction model is based on the following three steps:

1. Calculate the piston resonant frequency  $\omega_n$  (equation (4)).
2. Calculate the piston amplitude for given speed (equation (11)) with offset speed  $U' = 0.35\omega_n l_m$ .
3. Predict the ship resistance increase ( $\Delta CTS$ ) using the linear relationship between oscillation amplitude and resistance increase.



Step 1) in the prediction model applies the moonpool geometry (length, draft and width). Using the geometry draft over length ratio and Figure 10, the Strouhal number at maximum oscillation amplitude can be obtained and thus the forward speed at which resonance stops. If the velocity is above the peak value, an almost linear trend toward  $(1/St) = 0.85$  approximates the amplitude well. Step 2) in the prediction model can be verified through the data presented in Figure 7 and Figure 10. Figure 10 includes (only) four data points for which maximum oscillation amplitudes were measured. For consistency these data points are positioned on the oscillation amplitude line of Figure 8. Step 3) can be made through the data presented in Figure 2, which relates the resistance coefficient increase and the actual  $A_{1/3}/d_m$  ratio.

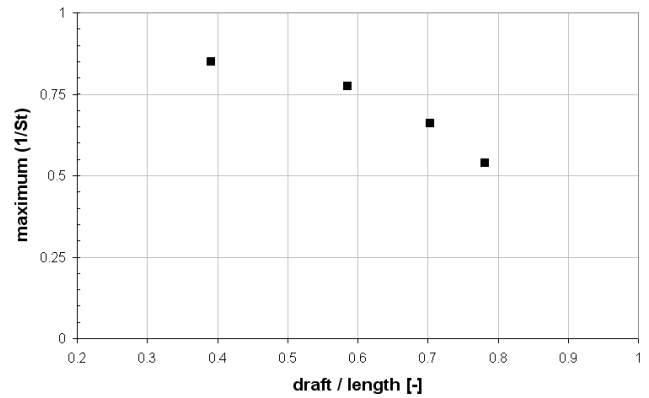


**Figure 10: Reduced velocity with maximum oscillation amplitude given moonpool draft over length ratio**

It is clear that a prediction model for added moonpool resistance is of great use for the designer. Given the limited data and the empirical bases for the model, the prediction is only a first estimate, but it might help to determine the speed-power curve with reasonable accuracy up to significant forward speed.

Unfortunately, the model test data is too limited to derive a 'similar' prediction for longer moonpools when sloshing resonance occurs. Based on the model test data, sloshing can be expected when  $D/L$  is lower than 0.35-0.39.

To verify the prediction model, three resistance curves are predicted for the moonpools that were used to construct the prediction model, and one resistance curve is calculated for an additional moonpool from a GustoMSC design, for which model tests were conducted at MARIN. The measured additional moonpool resistance and the predictions are given in Figure 11, showing a fair agreement. The  $L=24$  m moonpool is the additional moonpool configuration.

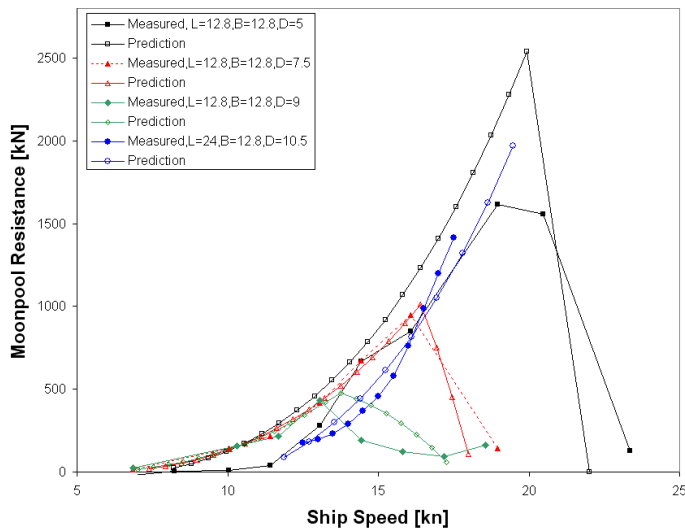


Figure 11: Resistance of the moonpool, measured and predicted (piston type oscillations of moonpool water column)

### SHIP MOTIONS

During the tests the model was free to heave and pitch and restricted in all other motion modes. In Figure 12 the water level amplitudes are presented versus the heave motion amplitudes. A strong correlation is found for both piston and sloshing mode oscillations. The sloshing amplitudes are calculated as the average of the amplitudes at the fore and aft end of the moonpool. As observed, sloshing oscillations have significant less influence on the heave motions than piston oscillations.

The ship heave and moonpool vertical motions were found out of phase. This indicates that additional vertical ship motions can decrease the piston oscillations and thereby the ship additional resistance. To verify this, several experiments were carried out with a captive model with trim and sinkage of the free moving model. A comparison is presented in Table 4. Apart from one entry in the table, the trend is that restraining the ship motions increases the water level oscillation amplitudes and increases the resistance by a significant value. The influence decreases with increasing moonpool length.

Table 4: Effect of ship motions on resistance

Geometry ratio length over beam [-]	Froude number [-]	effect due to captive ship motions		oscillation mode
		Resistance	Moonpool Oscillations	
1.0	0.13	+ 10.9 %	+ 14.2 %	piston
1.5	0.13	+ 8.5 %	+ 10.9 %	piston
	0.21	+ 7.9 %	+ 8.9 %	piston
2.0	0.13	+ 2.4 %	- 5.7 %	sloshing
	0.21	+ 5.8 %	+ 10.9 %	sloshing

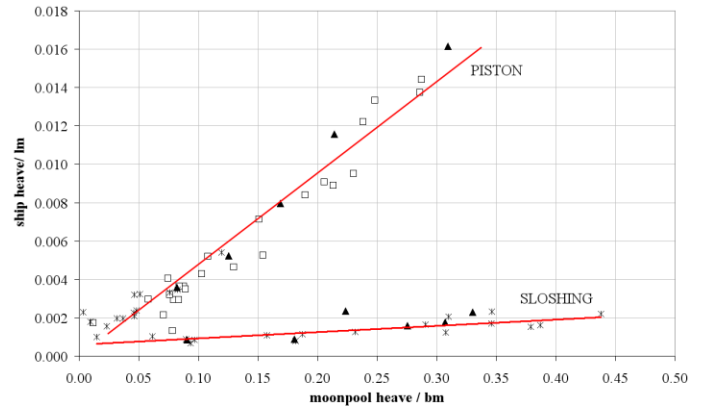


Figure 12: Relationship between vertical ship motions and vertical water motion amplitudes.

### CONCLUSIONS

The flow behaviour in a moonpool with free surface is complicated and can only be ‘easily’ visualized in terms of free surface behaviour. This paper sheds some light on the piston and sloshing modes. With increasing moonpool length over width, the sloshing oscillations were found to dominate above the piston mode, despite the fact that the piston mode always has a lower natural frequency. The natural frequency observed in model tests agrees well with theoretical predictions. Phase locking occurs, so that the resonant mode oscillations take place over a long speed range. The measured frequency varies thereby around the theoretical one.

The reduced velocity (inverse Strouhal number) is a useful quantity to assess moonpool oscillations. The oscillations in the tested moonpool configurations, being clean or modified, all start at  $1/St=0.35$  and the oscillations vanish at  $1/St=0.85$ . The oscillation amplitudes were found to increase linearly with the reduced velocity increase (line slope  $3\pi/16 \approx 0.589$ ). Fukuda derived this relationship, with a given damping coefficient for rectangular moonpools, and it agrees well with our measurement. For the tested resistance mitigation devices that reduce the ship resistance, the damping of the moonpool increases, which decreases this amplification factor.

The additional resistance from an in resonant moving water column is found to be very significant. Resistance increases in the order of 30% at low or moderate speed to as large as 100% at high forward speed. Careful assessment of the resistance is needed when a certain transit speed is required, and only model tests are used so far.

This paper presents an added resistance prediction model. The model is based on experimental data ([7] and [8]) of varying moonpool geometries. The validity of the resistance prediction model for moonpools with significant different geometry ratios cannot be verified extensively. In particular, the model assumes, and is limited to, piston type moonpool water oscillations.

The prediction model is applied to one earlier tested moonpool not used in the derivation of the prediction model. The predicted moonpool resistance curve versus speed agrees well with the measured calm water added resistance of that particular moonpool.

## REFERENCES

- [1] Gharib, M., Roshko, A. (1986): The effect of flow oscillations on cavity drag, *J. Fluid Mech.*, Vol. 177, pp. 501-530
- [2] Ibrahim, R. A. (2005): *Liquid Sloshing Dynamics, (Theory and Applications)*, Cambridge University Press
- [3] English, J.W. (1976): A means of reducing oscillations in drillwells caused by vessels' forward speed, *The Naval Architect*, May 1976, pp. 88-90
- [4] Fukuda, K. (1977): Behaviour of Water in Vertical Well with Bottom Opening of Ship and its Effects on Ship-Motion, *J. of the Soc. of Naval Architects of Japan*, Vol. 141, pp. 107-122 (in Japanese)
- [5] Molin, B. (2001): On the piston and sloshing modes in moonpools, *J. Fluid Mech.*, Vol. 430, pp. 27-50
- [6] Newman, N. (1977): *Marine Hydrodynamics*, The MIT Press, Cambridge
- [7] Cotteleer, A. (2000): Moonpool water motions caused by forward speed, MSc Thesis TU Delft
- [8] Tholen, H.J. (2008): Added resistance of moonpools at forward speed in calm water, MSc Thesis TU Delft, in preparation
- [9] Rockwell, D. and Naudasher, E. (1979): Self-sustained oscillations of impinging free shear layers, *Annual Review of Fluid Mechanics*, Vol. 11, pp. 67-94
- [10] Aalbers, A. B. (1984): The water motions in a moonpool, *Ocean Engineering*, Vol. 11, No. 6, pp. 557-579